








Amyloid Beta42 oligomers up-regulate the excitatory synapses by potentiating presynaptic release while impairing postsynaptic NMDA receptors

Andrea Marcantoni¹ , Maria Sabina Cerullo^{1,*} , Pol Buxeda¹, Giulia Tomagra¹ ,
Maurizio Giustetto^{2,3} , Giuseppe Chiantia¹ , Valentina Carabelli¹  and Emilio Carbone¹ 

¹Department of Drug Science and Technology, Torino University, Italy

²Department of Neurosciences / National Institute of Neuroscience, Torino University, Italy

³National Institute of Neuroscience-Italy, Turin, Italy

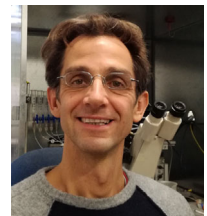
Edited by: David J. A. Wyllie & Jesper Sjöström

Key points

- NMDA receptors (NMDARs) are key molecules for controlling neuronal plasticity, learning and memory processes. Their function is impaired during Alzheimer's disease (AD) but the exact consequence on synaptic function is not yet fully identified.
- An important hallmark of AD onset is represented by the neuronal accumulation of Amyloid Beta42 oligomers (Abeta42) that we have recently shown to be responsible for the increased intracellular Ca^{2+} concentration through ryanodine receptors (RyRs).
- Here we characterized the effects of Abeta42 on NMDA synapses showing specific pre- and post-synaptic functional changes that lead to a potentiation of basal and synchronous NMDA synaptic transmission.
- These overall effects can be abolished by decreasing Ca^{2+} release from RyRs with specific inhibitors that we propose as new pharmacological tools for AD treatment.

Abstract We have recently shown that Amyloid Beta42 oligomers (Abeta42) cause calcium dysregulation in hippocampal neurons by stimulating Ca^{2+} release from ryanodine receptors (RyRs) and inhibiting Ca^{2+} entry through NMDA receptors (NMDARs). Here, we found that Abeta42 decrease the average NMDA-activated inward current and that Ca^{2+} entry through NMDARs is accompanied by Ca^{2+} release from the stores. The overall amount of intracellular Ca^{2+} concentration ($[Ca^{2+}]_i$) increase during NMDA application is 50% associated with RyR opening and 50% with NMDARs activation. Addition of Abeta42 does not change this proportion. We estimated the number of NMDARs expressed in hippocampal neurons and their unitary current. We found that Abeta42 decrease the number of NMDARs without altering their unitary current. Paradoxically, the oligomer increases the size of electrically evoked eEPSCs induced by NMDARs

Andrea Marcantoni received his PhD in Physiology in 2004. During his post-doctoral period he mainly worked on the Ca^{2+} -dependent modulation of various cellular functions. As a tenure-track researcher at the Department of Drug Science and Technology (DSTF) in Torino (Italy), in the last 5 years he has concentrated his interests on the role of voltage-gated Ca^{2+} channels on cell firing and neurotransmitter release in neurons and neuroendocrine cells. He is currently working on the pathological effects of accumulation of amyloid beta peptides on hippocampal neurons by focusing on their ability to induce Ca^{2+} dysregulation and impaired neuronal excitability and synaptic plasticity. He is now associate professor at the DSTF in Torino.



*Present address: Centre for Synaptic Neuroscience and Technology, Istituto Italiano di Tecnologia, Largo Rosanna Benzi 10, 16132 Genova, Italy and Department of Experimental Medicine, University of Genova, Viale Benedetto XV, 3, 16132 Genova, Italy.

activation. We found that this is the consequence of the increased release probability (p) of glutamate and the number of release sites (N) of NMDA synapses, while the quantal size (q) is significantly decreased as expected from the decreased number of NMDARs. An increased number of release sites induced by Abeta42 is also supported by the increased size of the ready releasable pool (RRPsyn) and by the enhanced percentage of paired pulse depression (PPD). Interestingly, the RyRs inhibitor dantrolene prevents the increase of PPD induced by Abeta42 oligomers. In conclusion, Abeta42 up-regulates NMDA synaptic responses with a mechanism involving RyRs that occurs during the early stages of Alzheimer's disease (AD) onset. This suggests that new selective modulators of RyRs may be useful for designing effective therapies to treat AD patients.

(Received 25 November 2019; accepted after revision 26 March 2020; first published online 4 April 2020)

Corresponding author A. Marcantoni, Department of Drug Science and Technology, Torino University, Corso Raffaello 30, 10125 Torino, Italy. Email: andrea.macantoni@unito.it

Introduction

The accumulation of amyloid beta oligomers (Abeta) derived from amyloid precursor protein (APP) processing induces neuronal Ca^{2+} dysregulation and synaptic dysfunction and is considered one of the better defined hallmarks of Alzheimer's disease (AD). Abeta oligomers cause dysregulation of Ca^{2+} homeostasis, neuronal cell death and consequent impairment of memory formation. Ca^{2+} dyshomeostasis induced by Abeta oligomers suggests some priority in the development of early strategies for the treatment of Ca^{2+} -mediated neuronal impairments. An uncontrolled increase of intracellular Ca^{2+} concentration ($[\text{Ca}^{2+}]_i$) may result from the alteration of different pathways of Ca^{2+} entry through the plasma membrane or Ca^{2+} release from Ca^{2+} stores. During the past 15 years, data have been accumulated concerning the impairment of both mechanisms of $[\text{Ca}^{2+}]_i$ increase during AD. Specifically, Abeta oligomers affect Ca^{2+} entry through NMDA receptors (NMDARs) (Snyder *et al.* 2005; Zhang *et al.* 2016) and/or voltage-gated calcium channels (VGCCs) (Nimmrich *et al.* 2008; Thibault *et al.* 2012; Wang & Mattson, 2013).

NMDARs are key regulators of memory formation (Costa *et al.* 2012). They are upregulated during AD onset, causing increased $[\text{Ca}^{2+}]_i$ (Danysz & Parsons, 2012), impaired synaptic function and accelerated neuronal death. VGCCs are also targeted by Abeta oligomers, but contrasting evidence suggests either an up- or down-regulation depending on the experimental procedure and brain region considered (Thibault *et al.* 2012; Wang & Mattson, 2013). The alternative mechanism of $[\text{Ca}^{2+}]_i$ increase associated with activation of ryanodine receptors (RyRs) and IP_3 receptors (IP_3 Rs) is impaired during AD onset (Mattson, 2010). RyRs and IP_3 Rs are not equally distributed along the endoplasmic reticulum (ER) membrane. IP_3 Rs are preferentially located in the somatic region and possibly involved in the control of Ca^{2+} -dependent excitatory phenomena while RyRs are preferentially expressed in the ER close to the synaptic sites

(Chakroborty *et al.* 2013) and are probably involved in the control of $[\text{Ca}^{2+}]_i$ governing synaptic activity. Considering our interest in the study of synaptic dysfunctions induced by Abeta42, here we focused on RyRs. These latter release Ca^{2+} following a calcium-induced calcium release (CICR) mechanism that requires their functional coupling to IP_3 Rs (Berridge, 2011), NMDARs (Goussakov *et al.* 2010; Sather & Dittmer, 2019) and VGCCs (Kim *et al.* 2007).

We have previously observed (Gavello *et al.* 2018) that spontaneous firing and intracellular Ca^{2+} homeostasis of the hippocampal neuronal network was altered after incubation with Abeta42 and concluded that a target of Abeta42 is represented by postsynaptic NMDARs. Starting from these considerations, here we performed patch-clamp and Ca^{2+} imaging recordings to test how the neurotoxic oligomer acts on NMDA-type glutamatergic synapses. We found that Abeta42 alter NMDA synapses by differently targeting pre- and postsynaptic sites. In particular, we found that Abeta42, besides reducing the number of postsynaptic NMDARs without altering their unitary current, increase the glutamate release probability, as expected by our previous observations regarding the effect of Abeta42 on intracellular Ca^{2+} homeostasis (Gavello *et al.* 2018). Using mean peak fluctuation analysis (MPFA) we next observed that Abeta42 increase both the release probability (p) and the number of release sites (N) of NMDA synapses, justifying the enhanced amplitude of NMDA-mediated eEPSCs. In line with this, through the analysis of cumulative eEPSCs during high-frequency stimulation (10 Hz) we found that Abeta42 increase the size of the ready-releasable pool (RRPsyn). Interestingly, administration of the RyR inhibitor dantrolene restores p and the size of eEPSCs to control values, suggesting that RyRs play a key role in the altered mechanisms of NMDA-type synaptic transmission induced by Abeta42. In conclusion, our data prompt a valuable description of how Abeta42 up-regulate NMDA synaptic responses with a mechanism involving RyRs (Danysz & Parsons, 2012) during the early stages of AD onset. This also suggests that

selective modulators of RyRs may be potential new drugs to treat AD patients.

Methods

Ethical approval

Ethical approval was obtained for all experimental protocols from the University of Torino Animal Care and Use Committee, Torino, Italy. All experiments were conducted in accordance with the National Guide for the Care and Use of Laboratory Animals adopted by the Italian Ministry of Health (Authorization DGSAF 00 11710-P-26/07/2017). All animals had free access from the shelter to water and food. Every effort was made to minimize the number of animals used. Pregnant female mice were obtained in our laboratory where the mating occurred. For removal of tissues, animals were exposed to a rising concentration of CO₂, leading to loss of consciousness and were then rapidly killed by cervical dislocation.

Cell culture

Hippocampal neurons were obtained from 18-day-old embryos of C57BL/6 mice (Envigo, San Pietro al Natisone, Italy). The embryos were rapidly decapitated before removal of tissues.

Hippocampus was rapidly dissected under sterile conditions, kept in cold Hanks' balanced saline solution (HBSS; 4°C) with high glucose, and then digested with papain (0.5mgml⁻¹) dissolved in HBSS plus DNase (0.1mgml⁻¹) as previously described (Allio *et al.* 2015). Isolated cells were plated at a final density of 1200 cellsmm⁻². Recordings were carried out at Days in Vitro (DIV) 18.

Patch clamp experiments

Patch electrodes, fabricated from thick borosilicate glasses (Hilgenberg, Mansfield, Germany), were pulled to a final resistance of 3–5 mΩ. Patch clamp recordings were performed in whole cell configuration using a Multiclamp 700-B amplifier connected to a Digidata 1440 and governed by the pClamp10 software (Axon Instruments, Molecular Devices, Sunnyvale, CA, USA).

Experiments were performed at room temperature (22–24°C) in whole cell configuration and acquired with sample frequency of 10 kHz. eEPSCs were filtered at half the acquisition rate with an eight-pole low-pass Bessel filter. Recordings with leak current > 100pA or series resistance > 20MΩ were discarded. Analysis was performed with Clampfit software (Axon Instruments).

Noise analysis on mEPSCs was performed with Mini-Analysis software (Synaptosoft, Decatur, GA, USA).

Voltage clamp

For currents dependent on NMDA administration (I_{NMDA}), recording neurons were held at -70 mV (V_h) for the entire duration of the experiments.

NMDA-dependent EPSCs following spontaneous action potentials (APs) or electrical stimulation were recorded by holding neurons at voltages of between -70 and $+50$ mV. eEPSCs were recorded by delivering presynaptic electrical stimuli through a glass pipette (1 μm tip diameter) filled with Tyrode's solution and placed in contact with the soma of a presynaptic neuron in a loose-seal configuration. The minimum amplitude (10–45 μA) of current pulses of 0.1 ms duration was generated by an isolated pulse stimulator (model 2100; A-M Systems, Carlsborg, WA, USA). Postsynaptic neurons were held at potentials comprised between -70 and $+50$ mV according to the typology of the experiment.

Calcium imaging

Hippocampal neurons plated on glass petri dishes were loaded with the fluorescent Ca²⁺ indicator Fura2-AM dye (3 μM) (Invitrogen, Molecular Probes) in the extracellular solution for 1 h. The fluorescent dye was then washed, and extracellular solution containing picrotoxin (100 μM) was replaced into the Petri dish. The inverted microscope used (Leica DMI3000B, Wetzlar, Germany) was equipped with a short-arc xenon gas discharge lamp (Ushio, Cypress, USA). Alternating excitation wavelengths of 340 and 380 nm were obtained by a monochromator (Till Photonics, Gräfelfing, Germany). The emitted fluorescence was measured at 500–530 nm. Images were projected onto a EMCCD camera (QuantEM:512SC, Photometrics, Tucson, AZ, USA) and stored every 200 ms. Spontaneous Ca²⁺ transients were recorded both in control conditions and after incubation with Abeta42 using Metafluor software (Molecular Devices) for data acquisition. The relative change in fluorescence ($\Delta F/F$) was measured considering the peak of Ca²⁺ transients.

Solutions and drugs

For voltage clamp recordings the external solution contained (in mM): 130 NaCl, 1.8 CaCl₂, 10 Hepes, 10 glucose and 1.2 glycine (pH 7.4). Where indicated we used the external Tyrode's Standard solution containing (in mM): 2 CaCl₂, 130 NaCl, 2 MgCl₂, 10 Hepes, 10 glucose and 4 KCl (pH 7.4). The internal solution contained (in mM): 90 CsCl, 8 NaCl, 20 TEACl, 10 EGTA, 10 glucose, 1 MgCl₂, 4 ATP, 0.5 GTP and

15 phosphocreatine (pH 7.4 with CsOH). For blocking synaptic currents due to the activation of glutamatergic AMPARs and GABAergic synapses (GABA_A receptors) we added respectively 6,7-dinitroquinoxaline-2,3-dione, DNQX (20 μ M, Sigma-Aldrich, St Louis, MO, USA) and picrotoxin (100 μ M, Sigma-Aldrich). Tetrodotoxin (TTX, 0.3 μ M, Tocris Bioscience, Bristol, UK) was added to block voltage-gated Na⁺ channels. Dantrolene (10 μ M, Sigma-Aldrich) was acutely administrated to neurons for 2 min before the beginning of the recordings in order to block RyRs. (2R)-amino-5-phosphonopentanoate, APV (50 μ M, Sigma Aldrich) was added to block NMDARs.

For calcium imaging experiments the external solution was the same used as in voltage clamp experiments with added picrotoxin, DNQX and TTX.

The neuron was constantly superfused through a gravity system that allowed a rapid change (50–60ms) of the solutions and the recording of I_{NMDA} following NMDA administration at different concentrations. During these experiments NMDA was administered to neurons until I_{NMDA} reached the maximum amplitude.

Abeta42 (Sigma-Aldrich) was dissolved in 1% ammonium hydroxide solution and stored at -20°C at a concentration of 1 mM. As previously described (Gavello *et al.* 2018), neurons were incubated with Abeta42 (1 μ M) for 48 h before the beginning of the experiments

Statistics

Data are given as mean \pm SD for n number of cells. The normal distribution of experimental data was assessed through the D'Agostino Pearson's normality test. Unless differently specified, the statistical significance of our data has been evaluated by considering two sample groups normally distributed and applying the paired or unpaired Student's t test. Otherwise, in case of more than two normally distributed sample groups, the one-way ANOVA test followed by Bonferroni's test was used. In case of two sample groups not normally distributed we used the non-parametric Mann–Whitney's U test. The Kruskal–Wallis's test followed by Dunn's *post hoc* test has been used in case of more than two sample groups not normally distributed. Data were statistically significant at $p < 0.05$.

Results

Abeta42 oligomers decrease NMDAR inward currents without impairing ligand-receptor binding affinity

Networks of primary cultured hippocampal neurons are known to generate spontaneous bursts of action potentials (APs) (Bacci *et al.* 1999; Gavello *et al.* 2012) that are modulated by inhibitory and excitatory synapses

(Gavello *et al.* 2018). Glutamatergic synapses dependent on NMDARs activation (NMDA synapses) are involved in the modulation of spontaneous network excitability and inhibited by Abeta42 oligomers (Gavello *et al.* 2018). As a first approach, we tested whether this inhibition affected pre- or postsynaptic mechanisms. For this, we compared pre- or postsynaptic mechanisms. For this, we compared currents activated by application of exogenous NMDA in control *versus* Abeta42-treated neurons. Patch clamp experiments, performed by holding neurons at $V_h = -70$ mV, showed that 50 μ M NMDA induces a mean I_{NMDA} of 352.3 ± 288.6 pA ($n = 31$) that is reduced to 117.3 ± 72.3 pA ($n = 23$) by 1 μ M Abeta42 (** $p < 0.001$, Mann–Whitney test) (Fig. 1A–C). Significant reductions of I_{NMDA} amplitude ($*p < 0.05$, ** $p < 0.01$, Mann–Whitney test) were observed by varying the NMDA concentration from 20 to 300 μ M (Fig. 1C).

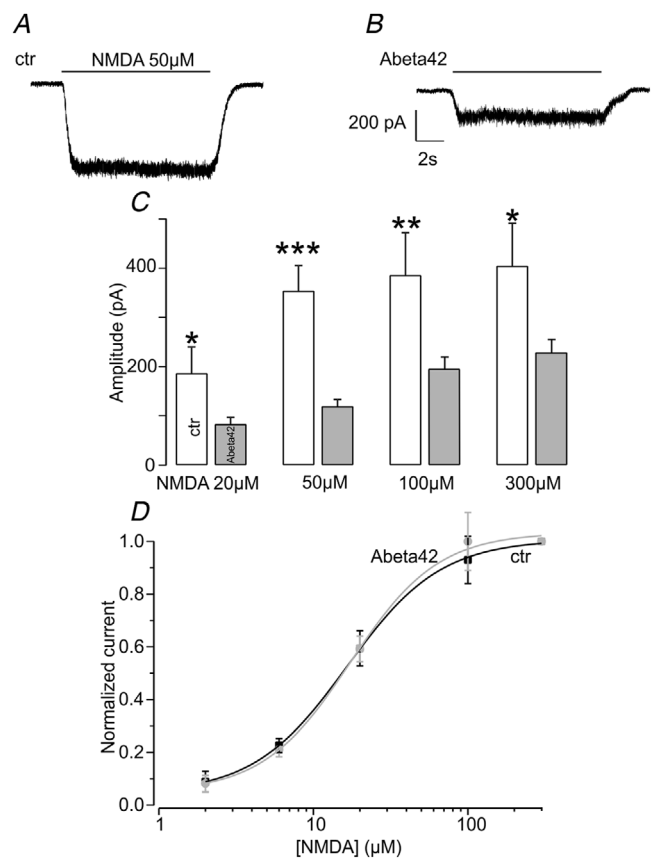


Figure 1. Abeta42 reduce I_{NMDA} without altering NMDAR binding affinity

A, representative inward current activated by NMDA (50 μ M) recorded in patch clamp experiments on primary cultured hippocampal neurons by holding neurons at $V_h = -70$ mV. B, when neurons were incubated for 48 h with Abeta42 the current activated by NMDA administration was significantly inhibited. C, bar graphs summarizing the inhibitory effect induced by Abeta42 on inward currents activated by different concentrations of NMDA (from 20 to 300 μ M). D, dose–response sigmoid curve of the current activated by NMDA (from 2 to 300 μ M) is not affected by Abeta42.

Further experiments were performed by decreasing the Abeta42 concentration to 10 nM. Under this condition (not shown), we still observed that 10 nM Abeta42 reduced I_{NMDA} by 30% with 50 μM NMDA (from 710.7 ± 314.3 pA, $n = 17$, to 486.9 ± 293.8 pA, $n = 15$; *** $p < 0.001$, Mann–Whitney test). Plots of normalized I_{NMDA} versus NMDA concentration ($[\text{NMDA}]$, from 2 to 300 μM) exhibited dose–response relationship fitted by the equation $y = A_2 + \frac{A_1 - A_2}{1 + (x/x_0)^p}$ of similar steepness (p) and IC_{50} (see legend to Fig. 1D). The p values were 1.4 ± 0.4 in control (ctr) and 1.5 ± 0.4 in the presence of Abeta42 and the IC_{50} values were 17.3 ± 3.3 μM in control and 16.5 ± 3.9 μM with Abeta42 (Fig. 1D). We thus concluded that Abeta42 inhibit the I_{NMDA} amplitude without significantly affecting the stoichiometry and the ligand–receptor binding affinity.

Abeta42 decrease the number of NMDARs without altering their single-channel conductance

To understand how Abeta42 inhibit postsynaptic NMDA-activated currents we estimated the mean number of functioning NMDARs and their single-channel conductance both in control and in the presence of Abeta42, by comparing the variance (σ^2) of I_{NMDA} stationary noise (Sigworth, 1980). We calculated σ^2 for periods of 2 s during stationary conditions of I_{NMDA} and plotted the values as a function of the average I_{NMDA} amplitudes generated by increased concentrations of NMDA (Traynelis & Jaramillo, 1998). The relationship between σ^2 and I_{NMDA} is described by the following parabolic equation: $\sigma^2 = iI - I^2/n$, where i is the unitary current of NMDARs, n the number of activated NMDARs and I is the mean I_{NMDA} amplitude. We observed drastically lower values of I_{NMDA} amplitudes and σ^2 in neurons incubated with Abeta42 compared to control neurons (Fig. 2A–D). The fit with the above parabolic function gave a significantly decreased number of NMDARs (n) with Abeta42 (from 454 ± 255 to 249 ± 133 after incubation with Abeta42; * $p < 0.05$, Mann–Whitney test) (Fig. 2E) and nearly similar values for the single-channel unitary current (i) (1.9 ± 0.7 pA in control neurons and 1.8 ± 0.6 pA in cells treated with Abeta42; $p = 0.58$, Mann–Whitney test) (Fig. 2F). The corresponding single-channel conductance values of NMDARs were 19 and 20 pS, respectively in controls and Abeta42-treated neurons calculated assuming a reversal potential (V_{rev}) of +25 mV that was determined from the reversal potential of EPSCs (Fig. 5A). Finally, we estimated the maximum open probability of NMDA channels $p = I/(N \times i)$ (Traynelis & Jaramillo, 1998) and found no significant changes ($p = 0.83$) between control (0.50 ± 0.18) and Abeta42-treated neurons (0.52 ± 0.17) (Fig. 2G).

Abeta42 decrease $[\text{Ca}^{2+}]_i$ but preserve the Ca^{2+} -induced Ca^{2+} release coupling between NMDARs and RyRs

Having previously shown that Abeta42 increase the amount of $[\text{Ca}^{2+}]_i$ by targeting RyRs (Gavello *et al.* 2018), we wondered whether NMDARs, known to be permeable to Ca^{2+} (Emptage *et al.* 1999), were involved in this process. Using Ca^{2+} imaging we quantified the $[\text{Ca}^{2+}]_i$ increase induced by NMDA administration (50 μM) and its modulation by Abeta42, knowing that the mechanism of Ca^{2+} -induced Ca^{2+} release (CICR) through RyR activation is upregulated by Abeta42 (Gavello *et al.* 2018). We observed a marked increase of $[\text{Ca}^{2+}]_i$ during NMDA application (Fig. 3A) that was fully prevented by the extracellular Ca^{2+} -free solution (0 Ca^{2+}). In control neurons (Fig. 3B), NMDA induced an approximately 8-fold increase of $[\text{Ca}^{2+}]_i$ ($\Delta F/F = 7.9 \pm 5.7$, $n = 25$) that was nearly halved by Abeta42 ($\Delta F/F = 4.7 \pm 2.3$, $n = 33$; * $p < 0.05$, Mann–Whitney test) (Fig. 3B–D).

To quantify the involvement of RyRs in the CICR mechanism triggered by NMDA, we inhibited RyRs by applying 10 μM dantrolene (Zhao *et al.* 2001). Surprisingly, in control and Abeta42-treated neurons dantrolene reduced to nearly half the NMDA-induced $[\text{Ca}^{2+}]_i$ increase. $\Delta F/F$ decreased from 7.9 ± 5.7 to 3.7 ± 2.6 ($n = 33$; * $p < 0.05$, Kruskal–Wallis test) in control (Fig. 3B–D) and from 4.7 ± 2.3 to 2.4 ± 1.7 ($n = 31$; * $p < 0.05$, Kruskal–Wallis test) in Abeta42-treated neurons. These results confirm that the NMDA-mediated $[\text{Ca}^{2+}]_i$ increase is nearly 50% associated with a CICR mechanism that involves RyRs and that this proportion is not altered by Abeta42. In fact, the $[\text{Ca}^{2+}]_i$ increase associated with the RyRs is 40% of the total in control and increases to 49% with the oligomers. In addition, despite the fact that Abeta42 potentiate Ca^{2+} released from RyRs (Lazzari *et al.* 2014; Gavello *et al.* 2018), the overall effect induced by Abeta42 on the $[\text{Ca}^{2+}]_i$ following NMDAR activation is reduced.

Abeta42 increase the number of release sites and the probability of release of NMDA synapses

To gain further insight into the effects of Abeta42 on glutamatergic NMDA synapses, we measured the amplitude of eEPSCs by holding neurons at +20 mV and varying the extracellular concentration of CdCl_2 (6 to 2 μM) and CaCl_2 (2 to 5 mM) to increase the release probability and thus increase eEPSCs amplitudes (Fig. 4A) (Clements & Silver, 2000). By comparing the eEPSC amplitudes (Fig. 4A, C, E) with those measured in neurons incubated with Abeta42 (Fig. 4B, D, F), we found that the oligomers significantly increased the mean eEPSC amplitude (from 214.4 ± 97.7 pA, $n = 14$, to

343.5 ± 169.1 pA, $n = 19$, $*p < 0.05$, in the presence of 2 mM CaCl_2) (Fig. 4G). We next performed MPFA to estimate the number of release sites (N), the quantal size (q) and the release probability (p) of glutamatergic NMDA synapses (Silver *et al.* 1998;

Clements & Silver, 2000; Baldelli *et al.* 2005). A parabolic function ($\sigma^2 = AI_{av} - BI_{av}^2$) describes the relationship between the variance of eEPSC amplitude (σ^2) and their mean postsynaptic current amplitude values (I_{av}) (Fig. 4C, D). N was obtained from B ($N = 1/B$), while q was taken

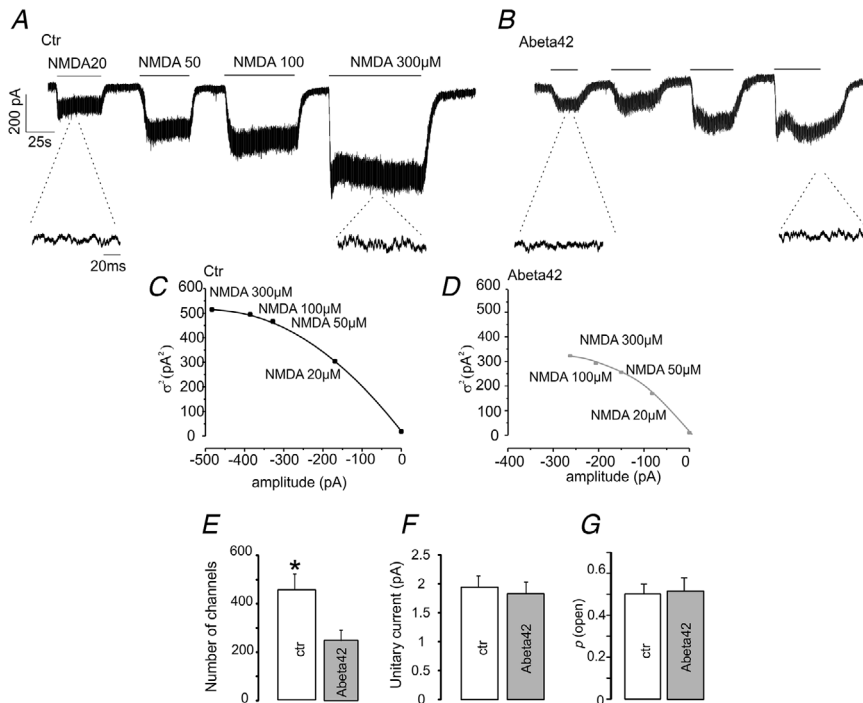


Figure 2. Abeta42 reduce the number of NMDARs without affecting their unitary current and open probability A, in control neurons NMDA administration activates inward currents of increased amplitude depending on the increased concentration of the agonist (from 20 to 300 μM). The insets show the noise signal that increases together with the increased current amplitudes. B, Abeta42 decrease the amplitude of inward currents activated by increasing concentrations of NMDA as well as the noise signal. C and D, representative parabolic relationship between the variance (σ^2) of the noise signal and mean of the inward current activated by NMDA in control neurons (C) and in the presence of Abeta42 (D). E, bar graph summarizing the significant decrease of the average number of NMDARs induced by Abeta42, despite their unitary current (F) and open probability (G) remaining unchanged.

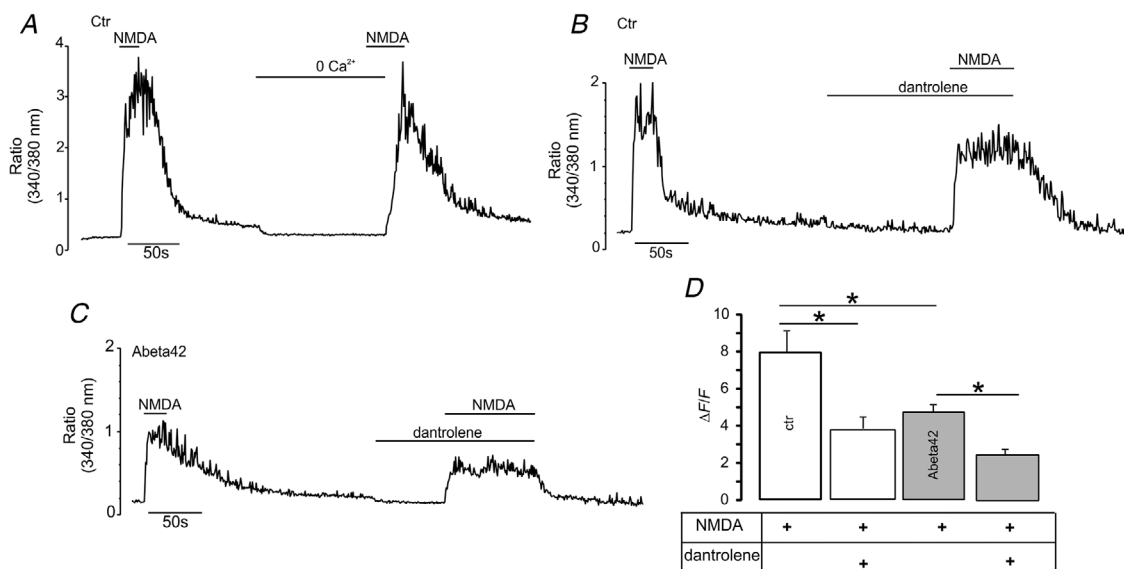


Figure 3. Abeta42 attenuates $[\text{Ca}^{2+}]_i$ preserving CICR coupling between NMDAR and RyRs

A, in calcium imaging experiments performed in control neurons, NMDA (50 μM) increases $[\text{Ca}^{2+}]_i$ when neurons are perfused with extracellular Tyrode's standard solution containing 2 mM Ca^{2+} , while this effect is reversibly abolished in the absence of Ca^{2+} (0 Ca^{2+}) in the extracellular medium. B, in control neurons the inhibition of RyRs through dantrolene (10 μM) halved the effect induced by NMDA. C, Abeta42 reduced by 50% the effect induced by NMDA on $[\text{Ca}^{2+}]_i$ and, similarly to control neurons, dantrolene halved the effect induced by NMDA. D, bar graphs summarizing the effect induced by NMDA (50 μM) on $[\text{Ca}^{2+}]_i$ in control and Abeta42-treated neurons. The related contribution of RyRs estimated by administration of dantrolene is shown.

as being equal to A . Finally, p was estimated considering that $I_{av} = Npq$. We observed that with Abeta42 N increased significantly from 136.6 ± 142.3 to 266.7 ± 191.9 ($*p < 0.05$) (Fig. 4H), while q decreased from 6.1 ± 2.7 to 3.9 ± 2.2 pA ($*p < 0.05$) (Fig. 4I) and p , measured in 2 mM $CaCl_2$, increased from 0.2 ± 0.06 to 0.3 ± 0.14 ($*p < 0.05$). Thus, MPFA demonstrates that Abeta42 increase the number of release sites and the probability of release while decreasing the quantal size of release. We

next focused on the presynaptic effects of Abeta42, possibly responsible for the observed increased rate of glutamate release and in turn for the increased p as well as eEPSC amplitude. As these experiments were performed in the absence of magnesium in the extracellular medium, we wanted to verify whether the effect induced by Abeta42 could be influenced by this ion. We therefore measured eEPSCs amplitude in the presence of Tyrode's standard solution containing 2 mM $MgCl_2$ by holding postsynaptic

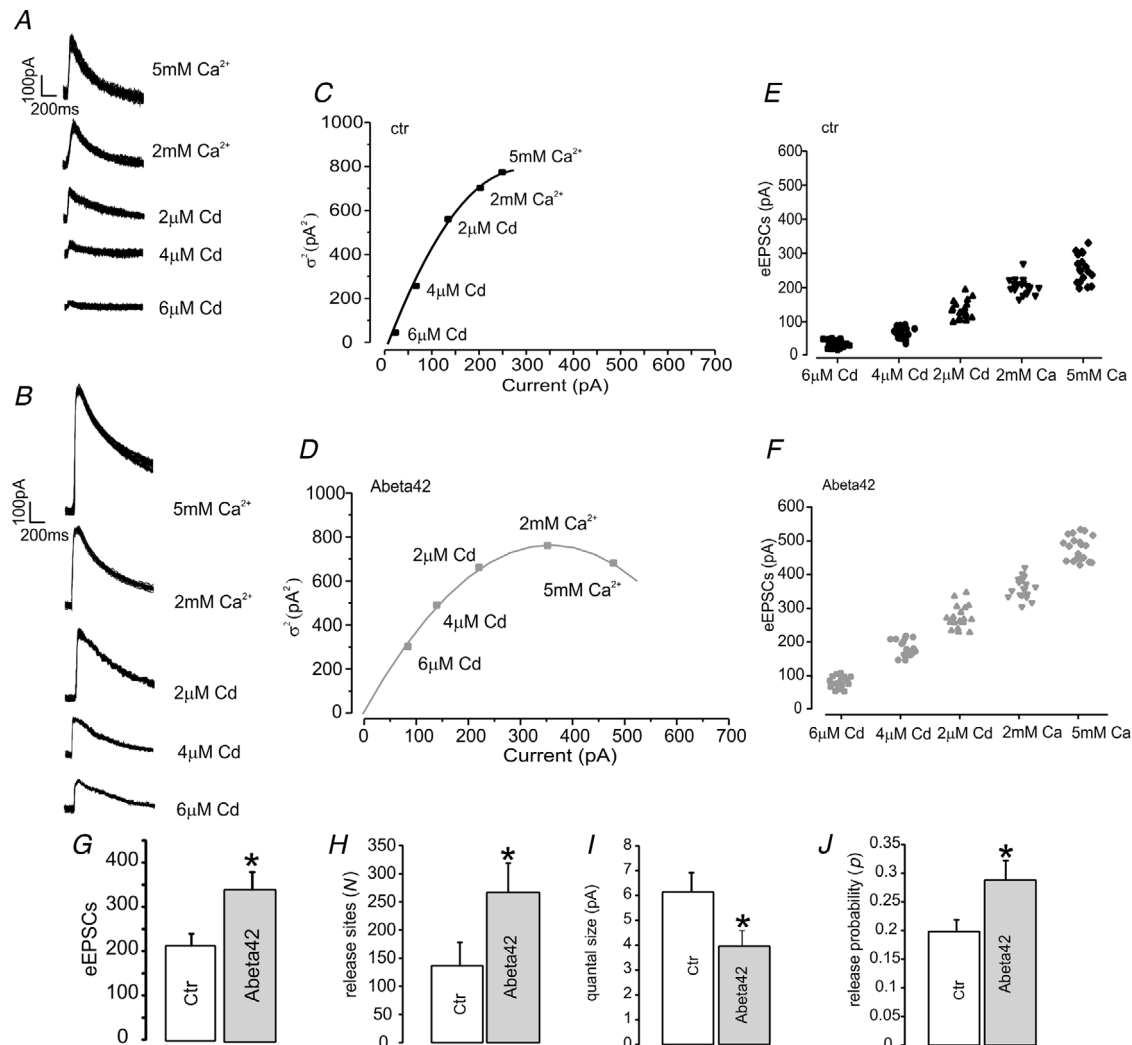


Figure 4. The number of release sites and probability of release is enhanced by Abeta42 in NMDA-sensitive synapses

A, 30 overlapping eEPSC traces dependent on NMDAR activation recorded in control neurons under different release probability conditions recorded by varying the concentrations of $CaCl_2$ or $CdCl_2$ in the external medium in order to change the release probability conditions. B, 30 overlapped eEPSC traces recorded after incubation of neurons with Abeta42 under different release probability conditions, similar to A. C, parabolic distribution of σ^2 as a function of eEPSC amplitude recorded in control neurons. D, Parabolic distribution of σ^2 as a function of eEPSC amplitude recorded in neurons incubated with Abeta42. E, peak amplitude of eEPSCs recorded in control neurons as a function of different concentrations of cadmium or calcium in the external medium. F, peak amplitude of eEPSCs recorded in neurons incubated with Abeta42 as a function of different concentrations of cadmium or calcium in the external medium. G, bar graph of the average amplitude of eEPSCs recorded at +20 mV with 2 mM Ca^{2+} in the external medium. H–J, number of release sites (H), quantal size (I) and release probability (J) of NMDA synapses in control neurons and in the presence of Abeta42.

neurons at +20 mV. Even in these experimental conditions we still observed that Abeta42 increased significantly the average eEPSC amplitude from 92.78 ± 58.37 pA ($n = 12$) to 332.69 ± 368.99 pA ($n = 12$) ($*p < 0.05$) (data not shown). We therefore concluded that magnesium does not interfere with the potentiating effect induced by Abeta42 on eEPSC amplitude.

Abeta42 increase the amplitude and frequency of spontaneous EPSCs

Because spontaneous firing of hippocampal neurons is impaired by Abeta42 and NMDARs are involved in this process (Gavello *et al.* 2018), we next determined how the oligomers affect the amplitude and frequency of EPSCs generated at NMDA synapses during spontaneous APs at V_h varying from -70 to $+50$ mV. The EPSC reversal potential was between $+20$ and $+30$ mV and Abeta42 increased significantly the average EPSC

amplitude at every potential (Fig. 5A, B). At $V_h = -70$ mV the average EPSCs amplitude in control neurons was -403.3 ± 158.6 pA ($n = 7$), while in the presence of Abeta42 it increased to -825.6 ± 288.7 pA ($n = 13$; $**p < 0.01$) (Fig. 5B, inset). When the inter-event intervals (IEIs) were considered, they were shorter and more regular (Fig. 5A) in Abeta42-treated neurons. IEIs in control and Abeta42-treated neurons had rather different Gaussian distributions. Control IEIs were best fitted with a double Gaussian function, with peaks respectively at 662.8 and 1841.3 ms (Fig. 5C, left panel), while IEIs in Abeta42-treated neurons were distributed according to a single Gaussian function with a peak at 1204 ms (Fig. 5C, right panel). The corresponding cumulative probability functions were significantly different (Kolmogorov–Smirnov (KS) test $***p < 0.001$) (Fig. 5D) and the same was for the coefficient of variation (CV) of IEIs that decreased markedly in Abeta42-treated neurons (0.59 ± 0.09 in

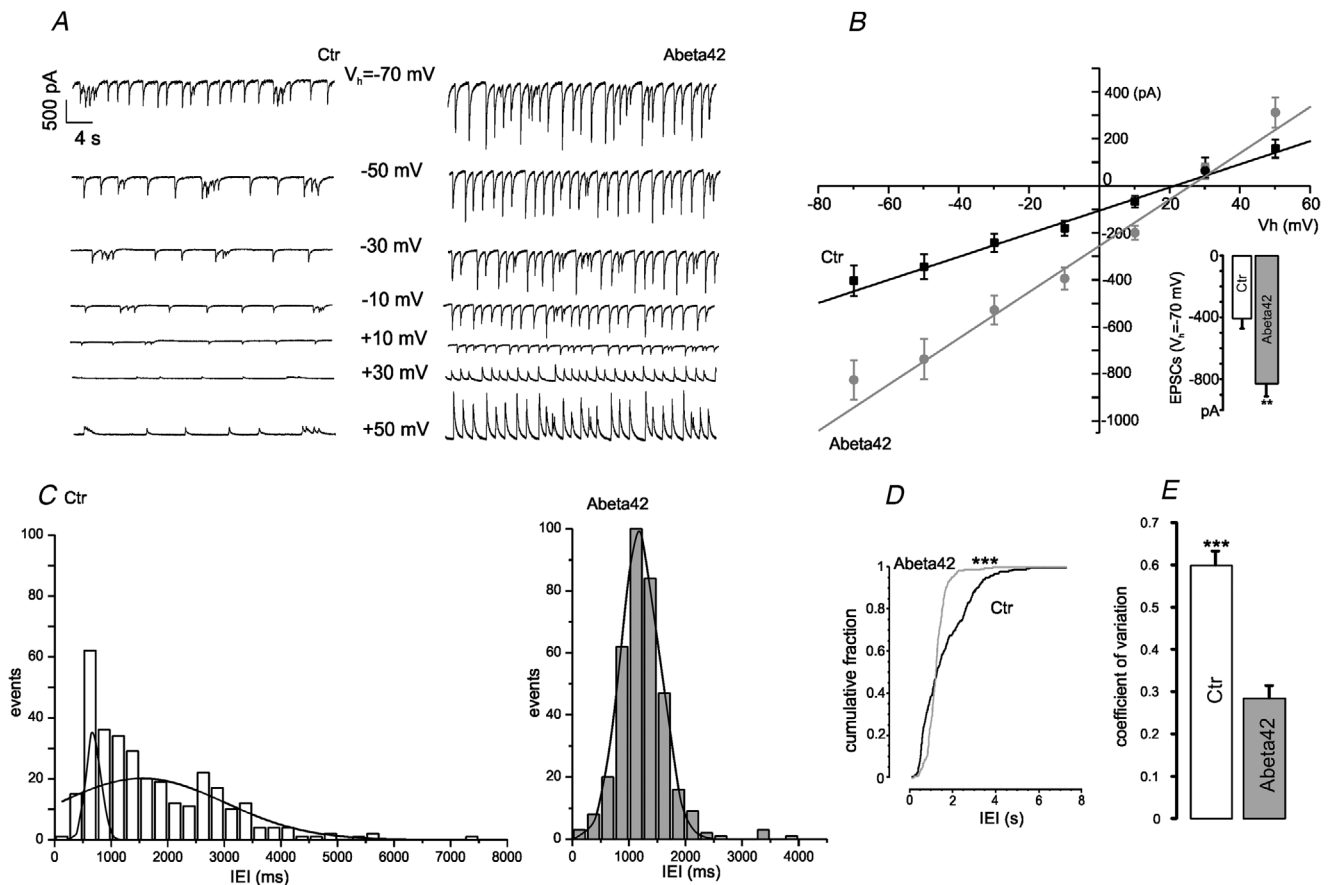


Figure 5. The amplitude and frequency of EPSCs is increased in Abeta42-treated neurons

A, spontaneous EPSCs recorded in control neurons and in the presence of Abeta42 by holding neurons at membrane potentials between -70 and $+50$ mV. B, mean EPSC amplitude evoked by spontaneous action potentials measured in control neurons and after administration of Abeta42 by holding neurons at membrane potentials between -70 and $+50$ mV. C, histograms showing the distribution of inter-event intervals (IEIs) in control neurons and in the presence of Abeta42. D, cumulative IEI distribution of spontaneous EPSCs in control neurons and in neurons incubated with Abeta42. E, bar graph of the coefficient of variation of IEIs in control neurons and in the presence of Abeta42.

control neurons vs. 0.28 ± 0.1 with Abeta42; *** $p < 0.001$) (Fig. 5E). Thus, Abeta42 besides increasing the amplitude of EPSCs, increases their frequency and regularity of occurrence.

Abeta42 increase synaptic depression during trains of stimuli

To better analyse the effects of Abeta42 on synaptic function we next assayed the NMDA-mediated synaptic response to high-frequency stimulation (10 Hz) for periods of 1.5 s (Schneeggenburger *et al.* 2002; Baldelli *et al.* 2005). Following this protocol, the amplitude of the eEPSCs was maximal during the first pulse of the train and then progressively depressed until reaching a constant value during the last 5–6 pulses, when the eEPSC amplitude reaches steady-state conditions (Fig. 6A, top). There was no sign of facilitation both in control and in Abeta42-treated cells. Nevertheless, it was evident that the eEPSC depression during the steady-state phase was more pronounced in Abeta42-treated neurons, despite the fact that the size of the first eEPSC was higher than in control

conditions (Fig. 6A, bottom). The increased synaptic depression in Abeta42-treated neurons was clearly visible when the normalized amplitude of eEPSCs was plotted vs. time (Fig. 6B, * $p < 0.05$) and fitted by a double exponential function with fast (τ_f) and slow (τ_s) time constants. We observed that τ_f and τ_s decreased in the presence of Abeta42, respectively from 0.97 and 32 ms in control to 0.30 and 13.4 ms with Abeta42.

We next focused on the cumulative profile of eEPSC amplitudes observing in control and in Abeta42-treated neurons a rapid rise of cumulative eEPSCs followed by a steady-state linear increase (Fig. 6C). This last linear phase reflects the equilibrium conditions between vesicle release and vesicle replenishment. According to Schneeggenburger *et al.* (2002) the intercept on the y -axis of the backward linear extrapolation of the last 5–6 points of the cumulative amplitude provides a probable estimate of the RRPsyn size generating the eEPSCs. The linear fits of the cumulative amplitudes show clearly an increased size of RRPsyn from 902.96 ± 596.1 pA ($n = 12$) in control to 1393.19 ± 467.07 pA ($n = 11$) in Abeta42-treated neurons (Fig. 6D). We could also estimate the size of the first eEPSCs and the RRPsyn and observed that Abeta42

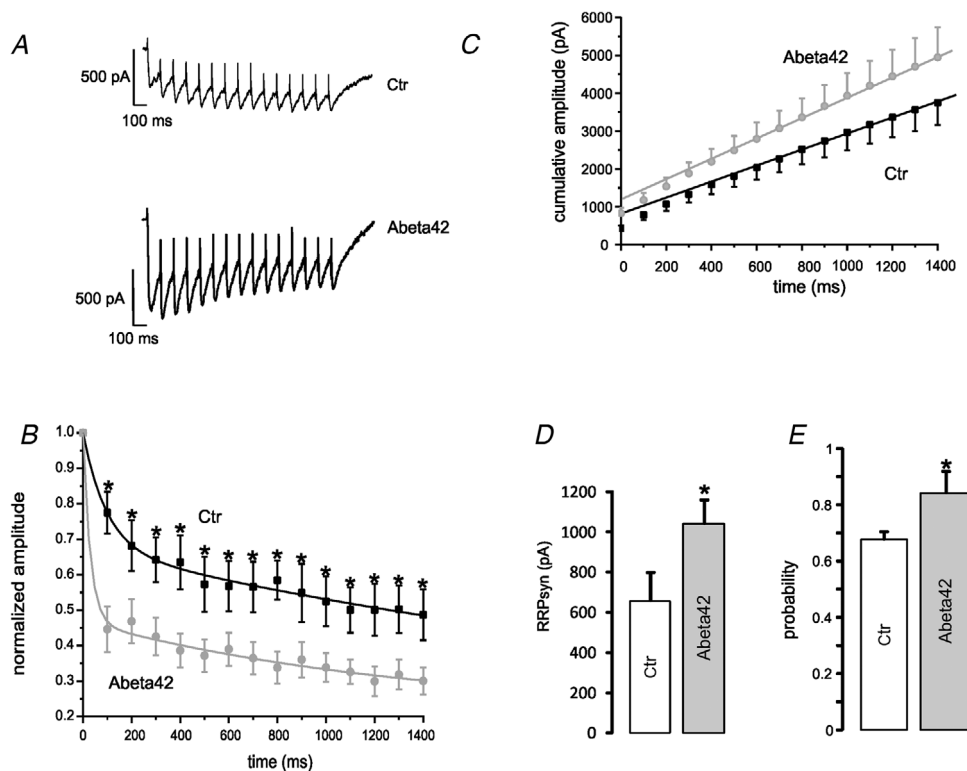


Figure 6. Synaptic depression during trains of stimuli is increased by Abeta42

A, eEPSCs recorded in control (top, black) and Abeta42- (bottom, grey) treated neurons by delivering repetitive constant pulses at 10 Hz for 1.5 s. B, normalized eEPSC amplitude as a function of time. C, cumulative amplitude distribution of eEPSCs as a function of time in control and after incubation of neurons with Abeta42. The final portion of the distribution follows a linear distribution. The intercept of the linear fit with the y -axis provides a quantification of ready releasable pool (RRPsyn) size. D and E, bar graphs of the size of RRP and release probability in control neurons and in neurons treated with Abeta42.

significantly increased p from 0.52 ± 0.07 to 0.63 ± 0.19 ($*p < 0.05$) (Fig. 6E).

Abeta42 increase the paired pulse depression of eEPSCs

To elucidate the presynaptic mechanism responsible for the increased eEPSCs amplitude induced by Abeta42, we tested whether the Abeta42-mediated increase of EPSCs influences the probability of Ca^{2+} -dependent neurotransmitter release. We therefore estimated the percentage of paired pulse depression (PPD) of eEPSCs by electrically stimulating presynaptic neurons with pairs of pulses separated by interpulse intervals of increasing duration (from 25 ms to 2 s) (Baldelli *et al.* 2002). The percentage of PPD plotted *versus* the interpulse interval duration decreased following a double exponential decay both in control and in Abeta42-treated neurons (Fig. 7A). Within the first 100 ms the PPD decreased from 55.4 ± 16.3 to $39.3 \pm 17.8\%$ ($n = 21$) in control (Fig. 7C and inset in Fig. 7A), while in Abeta42-treated neurons it decreased from initial higher values (72.8 ± 15.0 to $52.8 \pm 17.6\%$, $n = 13$; $*p < 0.05$). At interpulse intervals longer than

100 ms, PPD decayed with a slower time constant that was not significantly different between control and Abeta42-treated neurons. Because the magnitude of PPD at very brief interpulse intervals depends on the probability of release (p) (Dittman & Regehr, 1998), we can conclude that Abeta42 act presynaptically by increasing the probability of glutamate release.

When PPD was measured in the presence of dantrolene together with Abeta42, its value and decay time were comparable to that measured in control neurons (Fig. 7B, E). This suggests that the increased probability of glutamate release with Abeta42 is probably due to the amount of calcium released from RyRs that dantrolene effectively prevents. Finally, when comparing the average amplitude of the first eEPSC (Fig. 7C, D) at $V_h = -70$ mV we observed that Abeta42 cause a significant increase of the EPSC [from 319.8 ± 133.9 pA ($n = 13$) to 466.3 ± 191.9 pA ($n = 9$); $*p < 0.05$]. Interestingly dantrolene reduced the eEPSC amplitude to 389.7 ± 223.0 pA ($n = 13$; Fig. 7E), a value not significantly different ($p = 0.34$) from that measured in control conditions (319.8 ± 133.9 pA, $n = 13$; Fig. 7C). This observation together with what is shown in Fig. 7B indicates that RyRs inhibition prevents, at least

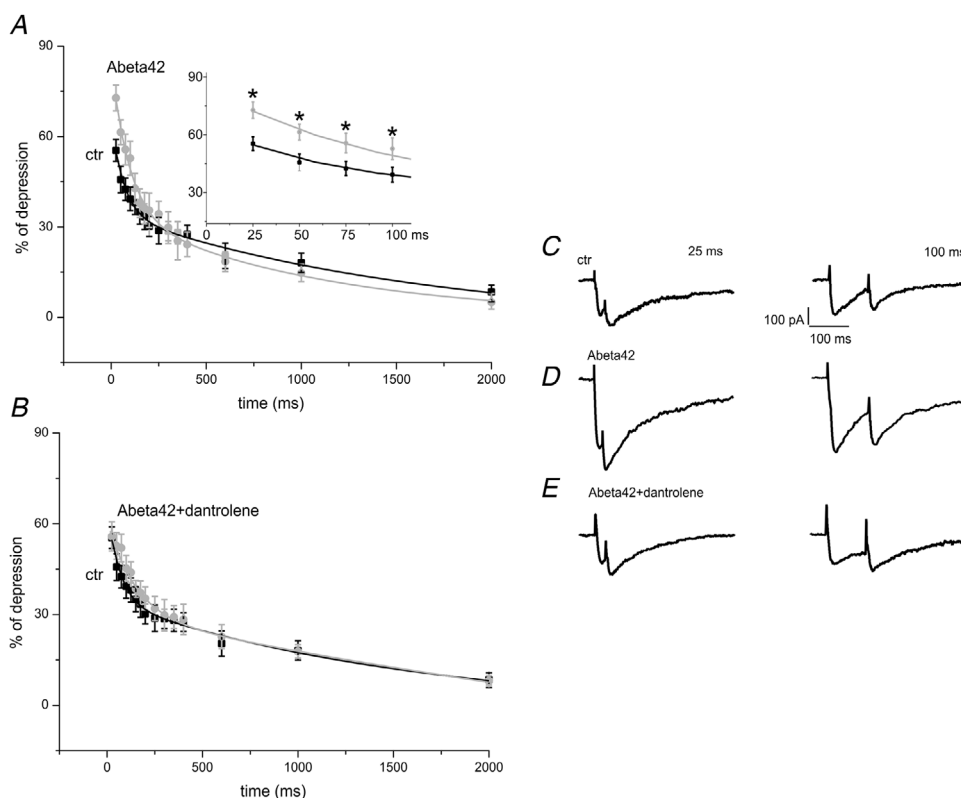


Figure 7. Dantrolene prevents the increased PPD of NMDA synapses induced by Abeta42

A, mean PPD (paired pulse depression) values plotted as a function of IPIs of different duration (between 25 and 2000 ms). The inset shows at higher magnification the PPD values calculated for IPIs between 25 and 100 ms. B, mean PPD values recorded after administration of dantrolene to neurons incubated with Abeta42. C–E, paired eEPSCs recorded by setting the IPI at 25 and 100 ms in control neurons (C), in neurons treated with Abeta42 (D) and in neurons treated with Abeta42 together with dantrolene (E).

in part, the synaptic effects induced by Abeta42 on NMDA synapses. Finally, to test whether the increased probability of glutamate release could also depend on an increasing amount of calcium entering through presynaptic VGCCs, in light of the well-documented potentiation of L-type calcium channels (LTCCs) observed in several models used for studying the mechanisms of AD onset (Navakkode *et al.* 2018), we measured eEPSC amplitude in control conditions and after administration of the LTCC blocker nifedipine (3 μ M) by holding postsynaptic neurons at +20 mV, without observing any significant effect in control neurons [eEPSC amplitude was 141.15 ± 88.50 pA ($n = 11$) in control and 162.12 ± 98.87 pA in the presence of nifedipine; $p = 0.27$]. When neurons were incubated with Abeta42 we found that in the majority of cells tested (11/14) nifedipine did not change the average eEPSC amplitude, which was 196.15 ± 96.53 pA in control and 176.30 ± 114.71 pA in the presence of nifedipine ($p = 0.4$). Of note, only in 20% (3/14) of cells incubated with Abeta42 we observed that nifedipine inhibited eEPSC amplitude by 37% [from 736.49 ± 117.44 to 461.65 ± 88.57 pA ($*p < 0.05$, data not shown)]. We suggest that Abeta42, besides increasing the amount of calcium released from RyRs, could be involved in the potentiation of presynaptic calcium influx through LTCCs.

Discussion

We have provided evidence that Abeta42 impair NMDAR-mediated glutamatergic synapses and targets both pre- and postsynaptic sites. Abeta42 inhibit the average current amplitude generated by NMDAR activation by decreasing the number of postsynaptic NMDARs without altering their unitary current and open probability. These inhibitory postsynaptic effects decrease the amount of calcium entering the cell through NMDARs, corroborating the hypothesis that Abeta42 inhibit neuronal function by targeting NMDA synapses (Gavello *et al.* 2018) and decreasing the number of NMDARs expressed on the membrane surface (Snyder *et al.* 2005), similarly to what has already been observed in aged brain (Tamaru *et al.* 1991). As these effects are accompanied by an increased amount of Ca^{2+} released through RyRs (Gavello *et al.* 2018; Navakkode *et al.* 2018) we conclude that the mechanisms responsible for the control of intracellular calcium concentration are differently affected by Abeta42. To clarify this issue we focused on EPSCs elicited by presynaptic electric stimulation or spontaneous APs. We unmasked a dual effect of Abeta42 that should not be ignored in the development of new therapies for AD treatment presently focused exclusively on NMDA synapses and based on the inhibition of NMDARs (Folch *et al.* 2017). We show that the postsynaptic inhibitory effect induced by Abeta42 on NMDA synapses contrasts with the

enhancing effect generated at the presynaptic site, where Abeta42 increase the eEPSCs amplitude by increasing the release probability of glutamate, the number of release sites and the size of the RRPsyn of NMDA synapses. Finally, we have pointed out that RyRs inhibition restores the average amplitude of eEPSCs to values comparable to those measured in control neurons and abolishes the increased PPD induced by Abeta42. In agreement with our previous results (Gavello *et al.* 2018), we confirm that inhibition of RyRs could be a promising strategy for treating early symptoms of AD.

Abeta42 decrease NMDA-activated inward current by reducing the number of postsynaptic NMDARs

To distinguish the pre- and postsynaptic effects induced by Abeta42 on NMDA glutamatergic synapses, we first focused on the postsynaptic effects on NMDARs. The inward current amplitude estimated during NMDA application is smaller if compared to the size of spontaneous EPSCs activated by synchronous glutamate release (Figs.1 and 5). This is in good agreement with the well-known property that NMDARs are more sensitive to glutamate than to NMDA (Monyer *et al.* 1992). Given this, we have shown that the oligomer decreases the expression of functionally active NMDARs without modifying the unitary current and open probability of the channel (Fig.2). Interestingly, the estimated NMDARs single-channel conductance (20pS) appears comparable to that measured in *Xenopus* oocytes (Wyllie *et al.* 1996) or obtained by using a similar approach (21–35pS) (Kohr *et al.* 1993) while is significantly reduced if compared to that measured in single-channel out-side-out patches of dissociated hippocampal neurons from neonatal rats (40–50pS) (Jahr & Stevens, 1987; Bekkers & Stevens, 1989). This difference is probably dependent on the type NMDAR subunits expressed in neurons (Wyllie *et al.* 1996) and by the analytical approach used, which in our experimental conditions is based on the indirect estimation of the single-channel parameters that can be affected by various errors. However, given the spread of a comparable error measured both in control and Abeta42-treated neurons, this does not limit the validity of the reported data.

Our findings are also in line with the idea of a downregulation of the non-amyloidogenic pathway of APP processing during AD (Snyder *et al.* 2005; Shankar *et al.* 2007) with consequent altered synaptic plasticity and neuronal survival (Hoey *et al.* 2009). The non-amyloidogenic pathway is upregulated by Ca^{2+} entering through NMDARs and the decreased Ca^{2+} influx through these receptors induced by Abeta42 contributes to exacerbate the early impairments induced by the oligomer. Abeta oligomers cause the inhibition

of long-term potentiation (Lambert *et al.* 1998) and, given the importance of Ca^{2+} influx through NMDARs in modulating spine formation, the decreased Ca^{2+} influx through NMDARs and consequent reduction of spine density induced by the oligomers (Shankar *et al.* 2007) are likely to be the triggering events of impaired learning and memory in AD. Here, we provide further support to an effective action of Abeta42 on postsynaptic NMDARs in determining hippocampal synaptic dysfunction by reducing the expression density of these receptors.

Abeta42 decrease the amount of $[\text{Ca}^{2+}]_i$ triggered by NMDARs activation but preserve the Ca^{2+} -induced Ca^{2+} release coupling to RyRs

Our findings on the $[\text{Ca}^{2+}]_i$ increase induced by NMDA correlate nicely with patch clamp experiments and show that I_{NMDA} inhibition by Abeta42 is accompanied by a proportional decrease of the Ca^{2+} entering through NMDARs. In neurons, a CICR coupling that triggers Ca^{2+} release from the ER via RyRs and IP_3 receptors (Emptage *et al.* 1999) accompanies this process. We aimed to correlate this result with our recently published findings on the overall increase of $[\text{Ca}^{2+}]_i$ induced by Abeta42 (Gavello *et al.* 2018) and wondered whether the CICR coupling triggered by NMDARs was impaired by Abeta42. Our data indicate that, independently of the presence of Abeta42, Ca^{2+} released from RyRs account for half of the total $[\text{Ca}^{2+}]_i$ increase and concluded that Abeta42 do not interfere with this mechanism of CICR. We therefore suggest that in contrast to previous observations by others (Goussakov *et al.* 2010), Ca^{2+} released from RyRs following NMDAR activation is not responsible for the increased $[\text{Ca}^{2+}]_i$ induced by Abeta42, possibly reflecting the different experimental model used in the experiments. We suggest that other Ca^{2+} sources responsible for potentiating Ca^{2+} release from RyRs are likely to be involved, such as the VGCCs that are down-regulated by Abeta42 (Gavello *et al.* 2018), or IP_3 receptors, known to be modulated by RyRs (Berridge, 2011) and to be impaired in some AD mouse models (Stutzmann *et al.* 2004). Alternatively, the existence of calcium leak phenomena coupled to RyRs should also be considered (Lacampagne *et al.* 2017).

Abeta42 increase the size of eEPSCs triggered by NMDAR activation

Using MPFA (Clements & Silver, 2000) we estimated the average number of synaptic release sites (N), the release probability (p) and the quantal size (q). Visual inspection of the shape of the parabolic variance–mean plot (Clements & Silver, 2000) reveals that the initial slope

of the parabola is lowered by Abeta42 (Fig. 4), suggesting a decreased q , which is in line with the decreased number of NMDARs estimated in Abeta42-treated neurons. Moreover, the degree of curvature of the same parabola is higher in the presence of Abeta42, confirming the increased p . This agrees with the analysis of cumulative EPSCs (Fig. 6) and increased PPD (Fig. 7). Finally, Abeta42 increase the size of the parabola that depends on N (Fig. 4H).

In addition, voltage-clamp experiments provide evidence that, in contrast to what we observed during direct application of NMDA (Fig. 1), neurons incubated with Abeta42 exhibit increased eEPSC amplitude. This is at variance with what we observed on AMPA synapses (Gavello *et al.* 2018) where eEPSC amplitudes are potentiated by Abeta42 only in the presence of RyRs or a BK channel inhibitor, indicating the existence of a ‘breaking’ action of calcium released from RyRs as already observed in 3xTg-AD mice (Chakroborty *et al.* 2009). This suggests different effects induced by increasing release of Ca^{2+} from RyRs on AMPA or NMDA synapses and underlie the need for an in-depth characterization of synaptic dysfunctions induced by Abeta42. A potentiating effect of Abeta42 on EPSC size is also evident by observing the larger amplitude, higher frequency and increased regularity of spontaneous EPSCs in the presence of Abeta42 (Fig. 5). All this suggests that Abeta42 is probably responsible for a presynaptic Ca^{2+} -dependent potentiating effect of glutamatergic synapses. Of particular interest is the increased regularity of spontaneous EPSCs induced by Abeta42. In this regard, it has been reported that in dopaminergic neurons the firing rate and regularity of firing are under the control of SK channels (Iyer *et al.* 2017). Indeed SK channels are considered important for controlling various brain function such as motor coordination (Walter *et al.*, 2006). Thus, it is likely that the increased $[\text{Ca}^{2+}]_i$ induced by Abeta42 activates robust SK currents that regulate spontaneous firing and synaptic function of hippocampal networks (Lancaster & Adams, 1986; Stocker *et al.* 1999).

Abeta42 increase the probability of glutamate release and reduce the ability of NMDA synapses to sustain prolonged stimulation

Study of the effects of Abeta42 on p has been investigated in details by measuring the paired pulse ratio (PPR) and the corresponding PPD. Hippocampal NMDA synapses are characterized by a net synaptic depression which can be regulated by either NMDAR desensitization (Mennerick & Zorumski, 1996) or activation of presynaptic GABA_B receptors (Huang & Gean, 1994). This short-term synaptic plasticity slows the firing rate of the hippocampal network. In this regard, we have previously shown (Gavello *et al.*

2018) that the spontaneous firing of cultured hippocampal neurons is characterized by bursts of APs of 600ms duration at 50Hz intraburst firing frequency, which corresponds to an average time interval of 20ms between APs. If we consider that Abeta42 significantly increase the PPD from 25 to 100ms, we expect a consistent inhibition of AP firing with Abeta42, in agreement with the reduced number of bursts and burst duration detected by micro electrode-arrays (MEAs) (Gavello *et al.* 2018). This inhibitory effect is in line with what has already been observed in Tg2576 mice overexpressing Abeta peptides (Marcantoni *et al.* 2014).

While our data reveal that Abeta42 increase the release probability (p) during paired pulses separated by 25–100 ms, it is evident that synapses treated with Abeta42 are unable to sustain prolonged stimulations during repetitive pulses at 10 Hz (Fig. 6). This occurs if the increased p induced by the oligomers determines a rapid emptying of vesicles, not followed by a fast replenishment as it occurs in hippocampal GABAergic interneurons after incubation with brain-derived neurotrophic factor (Baldelli *et al.* 2005). It should also be noted that the high-frequency stimulation (10 Hz) used in our voltage-clamp experiments is 5-fold lower than the effective AP frequency measured by MEAs during the train of APs within a burst (50 Hz) and probably underestimates the RRP_{syn} size while overestimating p . This suggests that in more physiological conditions the effect of Abeta42 on NMDA synapses during fast and prolonged stimulation would be more pronounced during the overall firing inhibition. Taken together, we can conclude that the potentiating presynaptic effects of Abeta42 reported here depend strongly on the increased amount of Ca^{2+} released from RyRs. The demonstration that calcium released from RyRs is involved in neurotransmitter release has been previously shown (Galante & Marty, 2003), as well as the existence of the ER calcium sensor STIM1 known to be involved in the control of the amount of calcium entering into neurons through LTCCs (Sather & Dittmer, 2019). In this regard it has been recently proposed that STIM1 inhibits calcium influx through LTCCs following calcium released from RyRs and that, through this mechanism, neurons could in turn modulate gene expression (de Juan-Sanz *et al.* 2017; Sather & Dittmer, 2019). These observations suggest that the recently described inhibition of somatic LTCCs following Abeta42 administration (Gavello *et al.* 2018) could depend on the increased amount of calcium released from RyRs, while the possible enhancement of presynaptic calcium influx through LTCCs described here agrees with the overall LTCC increase observed during the onset of several neurodegenerative diseases (Navakkode *et al.* 2018) and should be investigated in detail as well as the molecular mechanisms involved. A further confirmation of a presynaptic LTCC potentiation induced by Abeta42 could

be achieved by focusing on hippocampal slices where different neuronal populations can be selectively studied in order to evaluate the existence of a diverse sensibility of neurons to Abeta42 that could mask the effect of this peptide on LTCCs. These experiments would be useful for defining the calcium-dependent pathways responsible for the increased probability of neurotransmitter release. This latter, beside requiring an increased amount of calcium released through RyRs, could also be affected by an increased amount of calcium entry through VGCCs and by the activity of other ion channels such as BK potassium channels (Gavello *et al.* 2018). Finally the observation that dantrolene reverts the increased PPD induced by Abeta42 (Fig. 7) is in line with the previously reported effect of dantrolene in preventing the Abeta42-dependent increase of eEPSC amplitude, elevating $[Ca^{2+}]_i$ and inhibiting firing (Gavello *et al.* 2018). This effective action of RyR inhibitors on glutamatergic synapses suggests that a pharmacological therapy based on the development of selective RyRs blockers has a solid molecular basis.

References

- Allio A, Calorio C, Franchino C, Gavello D, Carbone E & Marcantoni A (2015). Bud extracts from *Tilia tomentosa* Moench inhibit hippocampal neuronal firing through GABAA and benzodiazepine receptors activation. *J Ethnopharmacol* **172**, 288–296.
- Bacci A, Verderio C, Pravettoni E & Matteoli M (1999). Synaptic and intrinsic mechanisms shape synchronous oscillations in hippocampal neurons in culture. *Eur J Neurosci* **11**, 389–397.
- Baldelli P, Hernandez-Guijo JM, Carabelli V & Carbone E (2005). Brain-derived neurotrophic factor enhances GABA release probability and nonuniform distribution of N- and P/Q-type channels on release sites of hippocampal inhibitory synapses. *J Neurosci* **25**, 3358–3368.
- Baldelli P, Novara M, Carabelli V, Hernandez-Guijo JM & Carbone E (2002). BDNF up-regulates evoked GABAergic transmission in developing hippocampus by potentiating presynaptic N- and P/Q-type Ca^{2+} channels signalling. *Eur J Neurosci* **16**, 2297–2310.
- Bekkers JM & Stevens CF (1989). NMDA and non-NMDA receptors are co-localized at individual excitatory synapses in cultured rat hippocampus. *Nature* **341**, 230–233.
- Berridge MJ (2011). Calcium signalling and Alzheimer's disease. *Neurochem Res* **36**, 1149–1156.
- Chakroborty S, Briggs C, Miller MB, Goussakov I, Schneider C, Kim J, Wicks J, Richardson JC, Conklin V, Cameransi BG & Stutzmann GE (2013). Stabilizing ER Ca^{2+} channel function as an early preventative strategy for Alzheimer's disease. *PLoS One* **7**, e52056.
- Chakroborty S, Goussakov I, Miller MB & Stutzmann GE (2009). Deviant ryanodine receptor-mediated calcium release resets synaptic homeostasis in presymptomatic 3xTg-AD mice. *J Neurosci* **29**, 9458–9470.

- Clements JD & Silver RA (2000). Unveiling synaptic plasticity: a new graphical and analytical approach. *Trends Neurosci* **23**, 105–113.
- Costa RO, Lacor PN, Ferreira IL, Resende R, Auberson YP, Klein WL, Oliveira CR, Rego AC & Pereira CM (2012). Endoplasmic reticulum stress occurs downstream of GluN2B subunit of *N*-methyl-D-aspartate receptor in mature hippocampal cultures treated with amyloid-beta oligomers. *Aging Cell* **11**, 823–833.
- Danysz W & Parsons CG (2012). Alzheimer's disease, beta-amyloid, glutamate, NMDA receptors and memantine—searching for the connections. *Br J Pharmacol* **167**, 324–352.
- de Juan-Sanz J, Holt GT, Schreier ER, deJuan F, Kim DS & Ryan TA (2017). Axonal endoplasmic reticulum Ca²⁺ content controls release probability in CNS nerve terminals. *Neuron* **93**, 867–881.e866.
- Dittman JS & Regehr WG (1998). Calcium dependence and recovery kinetics of presynaptic depression at the climbing fiber to Purkinje cell synapse. *J Neurosci* **18**, 6147–6162.
- Emptage N, Bliss TV & Fine A (1999). Single synaptic events evoke NMDA receptor-mediated release of calcium from internal stores in hippocampal dendritic spines. *Neuron* **22**, 115–124.
- Folch J, Busquets O, Ettcheto M, Sanchez-Lopez E, Castro-Torres RD, Verdaguer E, Garcia ML, Olloquequi J, Casadesus G, Beas-Zarate C, Pelegri C, Vilaplana J, Auladell C & Camins A (2017). Memantine for the treatment of dementia: a review on its current and future applications. *J Alzheimers Dis: JAD* **62**, 1223–1240.
- Galante M & Marty A (2003). Presynaptic ryanodine-sensitive calcium stores contribute to evoked neurotransmitter release at the basket cell-Purkinje cell synapse. *J Neurosci* **23**, 11229–11234.
- Gavello D, Calorio C, Franchino C, Cesano F, Carabelli V, Carbone E & Marcantoni A (2018). Early alterations of hippocampal neuronal firing induced by Abeta42. *Cerebr Cortex (New York, NY)* **28**, 433–446.
- Gavello D, Rojo-Ruiz J, Marcantoni A, Franchino C, Carbone E & Carabelli V (2012). Leptin counteracts the hypoxia-induced inhibition of spontaneously firing hippocampal neurons: a microelectrode array study. *PLoS One* **7**, e41530.
- Goussakov I, Miller MB & Stutzmann GE (2010). NMDA-mediated Ca²⁺ influx drives aberrant ryanodine receptor activation in dendrites of young Alzheimer's disease mice. *J Neurosci* **30**, 12128–12137.
- Hoey SE, Williams RJ & Perkinson MS (2009). Synaptic NMDA receptor activation stimulates alpha-secretase amyloid precursor protein processing and inhibits amyloid-beta production. *J Neurosci* **29**, 4442–4460.
- Huang CC & Gean PW (1994). Paired-pulse depression of the *N*-methyl-D-aspartate receptor-mediated synaptic potentials in the amygdala. *Br J Pharmacol* **113**, 1029–1035.
- Iyer R, Ungless MA & Faisal AA (2017). Calcium-activated SK channels control firing regularity by modulating sodium channel availability in midbrain dopamine neurons. *Sci Rep* **7**, 5248.
- Jahr CE & Stevens CF (1987). Glutamate activates multiple single channel conductances in hippocampal neurons. *Nature* **325**, 522–525.
- Kim S, Yun HM, Baik JH, Chung KC, Nah SY & Rhim H (2007). Functional interaction of neuronal Cav1.3 L-type calcium channel with ryanodine receptor type 2 in the rat hippocampus. *J Biol Chem* **282**, 32877–32889.
- Kohr G, De Koninck Y & Mody I (1993). Properties of NMDA receptor channels in neurons acutely isolated from epileptic (kindled) rats. *J Neurosci* **13**, 3612–3627.
- Lacampagne A, Liu X, Reiken S, Bussiere R, Meli AC, Lauritzen I, Teich AF, Zalk R, Saint N, Arancio O, Bauer C, Duprat F, Briggs CA, Chakroborty S, Stutzmann GE, Shelanski ML, Checler F, Chami M & Marks AR (2017). Post-translational remodeling of ryanodine receptor induces calcium leak leading to Alzheimer's disease-like pathologies and cognitive deficits. *Acta Neuropathol (Berl)* **134**, 749–767.
- Lambert MP, Barlow AK, Chromy BA, Edwards C, Freed R, Liosatos M, Morgan TE, Rozovsky I, Trommer B, Viola KL, Wals P, Zhang C, Finch CE, Krafft GA & Klein WL (1998). Diffusible, nonfibrillar ligands derived from Abeta1-42 are potent central nervous system neurotoxins. *Proc Natl Acad Sci USA* **95**, 6448–6453.
- Lancaster B & Adams PR (1986). Calcium-dependent current generating the afterhyperpolarization of hippocampal neurons. *J Neurophysiol* **55**, 1268–1282.
- Lazzari C, Kipanyula MJ, Agostini M, Pozzan T & Fasolato C (2014). Abeta42 oligomers selectively disrupt neuronal calcium release. *Neurobiol Aging* **36**, 877–885.
- Marcantoni A, Raymond EF, Carbone E & Marie H (2014). Firing properties of entorhinal cortex neurons and early alterations in an Alzheimer's disease transgenic model. *Pflugers Arch* **466**, 1437–1450.
- Mattson M. P. (2010) ER Calcium and Alzheimer's Disease: In a State of Flux. *Science Signaling*, **3** (114), pe10. <https://doi.org/10.1126/scisignal.3114pe10>.
- Mennerick S & Zorumski CF (1996). Postsynaptic modulation of NMDA synaptic currents in rat hippocampal microcultures by paired-pulse stimulation. *J Physiol* **490**, 405–417.
- Monyer H, Sprengel R, Schoepfer R, Herb A, Higuchi M, Lomeli H, Burnashev N, Sakmann B & Seeburg PH (1992). Heteromeric NMDA receptors: molecular and functional distinction of subtypes. *Science* **256**, 1217–1221.
- Navakkode S, Liu C & Soong TW (2018). Altered function of neuronal L-type calcium channels in ageing and neuroinflammation: Implications in age-related synaptic dysfunction and cognitive decline. *Ageing Res Rev* **42**, 86–99.
- Nimmrich V, Grimm C, Draguhn A, Barghorn S, Lehmann A, Schoemaker H, Hillen H, Gross G, Ebert U & Bruehl C (2008). Amyloid beta oligomers (A beta(1-42) globulomer) suppress spontaneous synaptic activity by inhibition of P/Q-type calcium currents. *J Neurosci* **28**, 788–797.
- Sather WA & Dittmer PJ (2019). Regulation of voltage-gated calcium channels by the ER calcium sensor STIM1. *Curr Opin Neurobiol* **57**, 186–191.
- Schneggenburger R, Sakaba T & Neher E (2002). Vesicle pools and short-term synaptic depression: lessons from a large synapse. *Trends Neurosci* **25**, 206–212.

- Shankar GM, Bloodgood BL, Townsend M, Walsh DM, Selkoe DJ & Sabatini BL (2007). Natural oligomers of the Alzheimer amyloid-beta protein induce reversible synapse loss by modulating an NMDA-type glutamate receptor-dependent signaling pathway. *J Neurosci* **27**, 2866–2875.
- Sigworth FJ (1980). The variance of sodium current fluctuations at the node of Ranvier. *J Physiol* **307**, 97–129.
- Silver RA, Momiyama A & Cull-Candy SG (1998). Locus of frequency-dependent depression identified with multiple-probability fluctuation analysis at rat climbing fibre-Purkinje cell synapses. *J Physiol* **510**, 881–902.
- Snyder EM, Nong Y, Almeida CG, Paul S, Moran T, Choi EY, Nairn AC, Salter MW, Lombroso PJ, Gouras GK & Greengard P (2005). Regulation of NMDA receptor trafficking by amyloid-beta. *Nat Neurosci* **8**, 1051–1058.
- Stocker M, Krause M & Pedarzani P (1999). An apamin-sensitive Ca^{2+} -activated K^{+} current in hippocampal pyramidal neurons. *PNAS* **96**, 4662–4667.
- Stutzmann GE, Caccamo A, LaFerla FM & Parker I (2004). Dysregulated IP3 signaling in cortical neurons of knock-in mice expressing an Alzheimer's-linked mutation in presenilin1 results in exaggerated Ca^{2+} signals and altered membrane excitability. *J Neurosci* **24**, 508–513.
- Tamaru M, Yoneda Y, Ogita K, Shimizu J & Nagata Y (1991). Age-related decreases of the *N*-methyl-D-aspartate receptor complex in the rat cerebral cortex and hippocampus. *Brain Res* **542**, 83–90.
- Thibault O, Pancani T, Landfield PW & Norris CM (2012). Reduction in neuronal L-type calcium channel activity in a double knock-in mouse model of Alzheimer's disease. *Biochim Biophys Acta* **1822**, 546–549.
- Traynelis SF & Jaramillo F (1998). Getting the most out of noise in the central nervous system. *Trends Neurosci* **21**, 137–145.
- Walter JT, Alvina K, Womack MD, Chevez C & Khodakhah K (2006). Decreases in the precision of Purkinje cell pacemaking cause cerebellar dysfunction and ataxia. *Nat Neurosci* **9**, 389–397.
- Wang Y & Mattson MP (2013). L-type Ca^{2+} currents at CA1 synapses, but not CA3 or dentate granule neuron synapses, are increased in 3xTgAD mice in an age-dependent manner. *Neurobiol Aging* **35**, 88–95.
- Wyllie DJ, Behe P, Nassar M, Schoepfer R & Colquhoun D (1996). Single-channel currents from recombinant NMDA NR1a/NR2D receptors expressed in *Xenopus* oocytes. *Proc Biol Sci* **263**, 1079–1086.
- Zhang Y, Li P, Feng J & Wu M (2016). Dysfunction of NMDA receptors in Alzheimer's disease. *Neurol Sci* **37**, 1039–1047.
- Zhao F, Li P, Chen SR, Louis CF & Fruen BR (2001). Dantrolene inhibition of ryanodine receptor Ca^{2+} release channels. Molecular mechanism and isoform selectivity. *J Biol Chem* **276**, 13810–13816.

Additional information

Competing interests

All authors declare no competing interests.

Author contribution

A.M. designed and performed experiments, and wrote the manuscript with input from all co-authors. S.C., P.B., G.C. and G.T. performed and analysed electrophysiological experiments. V.C., M.G. and E.C. critically revised the manuscript and contributed to design the experiments. All authors have read and approved the final version of the manuscript and agree to be accountable for all aspects of the work in ensuring that questions related to the accuracy or integrity of any part of the work are appropriately investigated and resolved. All persons designated as authors qualify for authorship.

Funding

This work was supported by the following projects: Project 2015FNWP34 (from Italian MIUR) to V.C. and A.M., CSTO165284 (from Compagnia di San Paolo) to V.C., and by local funds from Torino University to A.M., and FFABR funds (Fondo Finanziamento delle Attività Base di Ricerca) from Italian MIUR to A.M.

Acknowledgements

We are grateful to Dr Claudio Franchino for the preparation of cell cultures.

Keywords

Abeta42, calcium, dantrolene, L-type calcium channels (LTCCs), NMDA receptors (NMDARs), ryanodine receptors (RyRs), synapses

Supporting information

Additional supporting information may be found online in the Supporting Information section at the end of the article.

Statistical Summary Document